Eur Biophys J (2011) 40:937–946
DOI 10.1007/s00249-011-0709-0

ORIGINAL PAPER

Vibrational dynamics of bio- and nano-filaments in viscous solution subjected to ultrasound: implications for microtubules

Abdorreza Samarbakhsh · Jack A. Tuszynski

Received: 15 December 2010 / Revised: 20 April 2011 / Accepted: 28 April 2011 / Published online: 28 May 2011

Abstract In this paper, using a new analytical method, we solved the beam equation for a uniform bio- and nano-filament in a viscous solution. The filament is assumed to be attached at its two ends and driven by ultrasound plane waves. To obtain analytical solutions, we converted the beam equation to an equation that allows us the use of the method of separation of variables. We then reconstructed the solution of the original beam equation from the solution of the converted equation. Subsequently, we have used the parametric equations derived in this paper to investigate the resonance condition for a microtubule (MT) in an aqueous solution. We show that by using ultrasound plane waves, one cannot satisfy a resonance condition for MTs treated as rigid rods. In order to achieve resonance, a single mode of the MT vibration must be excited with a harmonic number larger than a threshold value found here. Single mode excitation not only helps to transfer a minimum amount of energy to the surrounding medium compared with multi-mode excitation, but it also allows for a simultaneous high amplitude and high mode quality that is impossible using plane waves. In order to overcome this difficulty, we propose to use an ultrasound generation device as a potential technical solution characterized by both frequency control and optimized energy transfer to the MT. Finally, the minimum required intensity of the ultrasound at the location of the MT in order to break it is shown to be on the order of 10^5 W/m^2, which corresponds to 170 dB.

Keywords Microtubule · Ultrasound · Vibration · Resonance · Bending elasticity

A. Samarbakhsh (✉) · J. A. Tuszynski
Department of Physics, University of Alberta, 11322 89 Ave, Edmonton, AB T6G 2G7, Canada
e-mail: asamar@ualberta.ca

A. Samarbakhsh · J. A. Tuszynski
Division of Experimental Oncology, Cross Cancer Institute, 11560 University Avenue, Edmonton, AB T6G 1Z2, Canada

Introduction

Ultrasound has been successfully used in medical imaging, and it is widely accepted today that high intensity focalized ultrasound (HIFU) may provide an effective noninvasive targeted modality that could help to deliver drugs in cells or else become an alternative to surgery in the treatment of both benign and malignant diseases. Kennedy et al. (2003) summarized the potential use of this technique in surgery from clinical trial data. For example, it was shown that HIFU was successful in reducing tumor size and pain and showed no adverse side effects for patients with pancreatic cancer (Wu et al. 2005). The efficiency of this technique was shown to depend on physical parameters such as frequency, intensity, the duration of the pulses, and time interval between pulses. For medical trials, the frequency range between 0.8 and 1.7 MHz and the intensity range between 1 and 20 KW/cm^2 were used. However, further studies are needed to understand the therapeutic mechanism of HIFU, to optimize the delivery of HIFU to the tumor site, and to decrease potential side effects. To understand the action of HIFU on cell structure, most studies thus far have been performed on either cultured or isolated cells (Miller et al. 1996; Hrazdira et al. 1998). In their studies on isolated cells, Hrazdira et al. (1998) have shown the partial disassembly of all components of the cytoskeleton and particularly microtubules (MTs) as a result of ultrasound exposure. In addition, it appears that

the effects of ultrasound depend on the phase of the cell cycle during which the exposure takes place (Hrazdira et al. 1998), with mitosis being the most sensitive phase. This disassembly was characterized by thinning of fibrous structures, their fragmentation and formation of granule-like structures. However, it is difficult to precisely interpret their experiments because when the experiment was performed on cells, other constituents of the cell were not properly monitored and analyzed (e.g., actin filaments). Therefore, it is necessary to study first of all isolated MTs and their behavior under the influence of externally applied ultrasound. Interestingly, the above-cited authors observed that ultrasound of intensities as low as 100 mW/cm^2 with a frequency of 0.8 MHz is enough to induce these damages. These studies showed that, depending on the physical parameters stated above, ultrasound damages or destroys cancer cells through three predominant mechanisms: (1) heating, (2) cavitation (repeated mechanical shocks intensified by formation of microbubbles; Kennedy et al. 2003), and most interestingly (3) mechanical shocks that break rigid filaments such as MTs without heating and cavitation.

Since MTs play a crucial role in cell division and since they have been shown to be strongly affected by ultrasound effects, in this study, we aimed to elucidate theoretically the vibrational dynamics of MTs in the absence of other cellular constituents and their behavior under the influence of externally applied ultrasound in situations where both cavitation and heating are negligible. In particular, we are interested in determining the existence of mechanical resonance conditions in terms of frequency, mode of application, and the energy needed to eventually break MTs since they play such an important role in the mitosis process. The study of ultrasound effects on isolated MTs is necessary to help understand its basic mechanisms of action on cells and tissues, and it is a fundamental question in nano-biophysics. Our ultimate goal is to improve the design and hence the use of HIFU for the treatment of cancer using noninvasive techniques. Recently, novel ultrasonic techniques, such as the acoustic lens (Spadoni and Daraio 2010), have been developed that offer additional capabilities of being able to focus the acoustic energy at specific locations. This, if properly fine tuned, can lead to oncologic applications of relevance to the research presented in this paper. In this work by introducing a new method we managed to analytically solve the equation of motion for the vibrational dynamics of an MT that is attached at its two ends. This is especially relevant for MTs during mitosis when they attach to chromosomes and centrosomes at the plus and minus ends, respectively. Below, we present the equations of motion used to model MTs subjected to ultrasound, their analytical solutions, and physical interpretation.

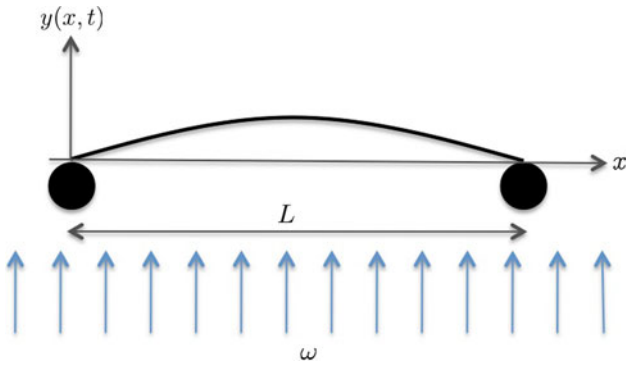

Fig. 1 Schematic illustration of a bio- or nano-filament that is attached to two beads at its ends. In the case of a microtubule, this can be regarded as an approximate representation of the MT during mitosis

Derivation of vibrational dynamics equations

In this section, starting with the beam equation (Rao 2004; Gere and Timoshenko 1991), we solve the vibrational differential equation of a bio- or nano-filament placed in a viscous solution under the influence of an ultrasound plane wave[1]. Our primary aim is to solve the problem parametrically and subsequently to find analytical solutions for different bio- or nano-filaments in an aqueous solution with a given viscosity subjected to an ultrasound source with an arbitrary frequency. In later sections, using the parametric solution that will be found in this section and the next, we will substitute the relevant values for an MT and analyze the results. Besides the fact that a parametric analytical solution is the best way to analyze the system, it will also be applicable to other cases by using the obtained solutions and substituting parameter values appropriate to the filament of interest. Here, we first derive the solution corresponding to free vibrations of the filament and then we find the response of the filament's vibrations when it is driven by an ultrasound source with different frequencies when the filament is attached at its two ends. This latter situation is a reasonable representation of MTs during mitosis.

Figure 1 shows a schematic drawing of a bio- or nano-filament with length L whose two ends are attached to the two beads that are trapped by laser tweezers (McDonald 2000; Neuman and Block 2004). The equation of motion of the filament, driven by a sinusoidal force density (force per

[1] The reason that we discuss the effects of a plane wave and not other types of waves in this paper is that due to the relatively short length of the bio- and nano-filaments (in particular MTs) compared to the distance between ultrasound source and the filament, we can approximate the waves used in the previous experiments on the filament (MT) as plane waves arriving at the location of the filament (MT).

unit length of the filament) with amplitude EIA[2] and angular frequency ω is

$$\frac{\partial^4 y(x,t)}{\partial x^4} + \frac{c_\perp}{EI}\frac{\partial y(x,t)}{\partial t} + \frac{\mu}{EI}\frac{\partial^2 y(x,t)}{\partial t^2} = A\sin(\omega t). \quad (1)$$

The second and the third terms on the left-hand side of the above equation come from the viscous drag force of the solution and the inertia of the filament, respectively. The term on the right-hand side represents the effect of the ultrasound source. Also, in Eq. 1 the viscous drag coefficient per unit length of the filament, flexural rigidity of the filament, and the linear mass density are denoted as $c_\perp$, EI, and μ, respectively.

Part 1: complementary solution or the free vibration case

To solve the above equation, we first find the solution for the homogeneous equation by setting the right-hand side of Eq. 1 to zero (to find the complementary function). Assuming that the solution for $y(x, t)$ is a separable function of x and t,

$$y(x,t) = X(x)Y(t), \quad (2)$$

and then substituting Eq. 2 into Eq. 1 and dividing the result by $X(x)Y(t)$, we obtain the following two eigenvalue equations:

$$\frac{d^4X(x)}{dx^4} = \alpha X(x), \quad (3)$$

$$\frac{d^2Y(t)}{dt^2} + \frac{c_\perp}{\mu}\frac{dY(t)}{dt} = -\alpha\frac{EI}{\mu}Y(t). \quad (4)$$

α is an arbitrary constant at this stage. As mentioned before, we solve the equation for a filament that has been attached at its two ends, which means the boundary conditions for Eq. 3 are

$$X(0) = X(L) = 0, \quad \frac{d^2X}{dx^2}\Big|_{x=0} = \frac{d^2X}{dx^2}\Big|_{x=L} = 0. \quad (5)$$

Applying the above boundary conditions to Eq. 3, we find the eigenfunctions and eigenvalues of Eq. 3 as

$$X_n(x) = \sin(\alpha_n^{1/4}x), \quad \alpha_n = \left(\frac{n\pi}{L}\right)^4. \quad (6)$$

Time dependence of the solution is a function of the mode number, n. This results in two main different situations[3] based on the mode number:

1. An over-damped case $\alpha_n\frac{EI}{\mu} < \left(\frac{c_\perp}{2\mu}\right)^2$
2. An under-damped case $\alpha_n\frac{EI}{\mu} > \left(\frac{c_\perp}{2\mu}\right)^2$.

The time-dependent solution is

$$Y_{c_n}(t) = \begin{cases} \exp\left(-\frac{c_\perp}{2\mu}t\right)\left[A_n\exp\left(\sqrt{\left(\frac{c_\perp}{2\mu}\right)^2 - \alpha_n\frac{EI}{\mu}}\,t\right) + B_n\exp\left(-\sqrt{\left(\frac{c_\perp}{2\mu}\right)^2 - \alpha_n\frac{EI}{\mu}}\,t\right)\right], & n \le n_c \\ C_n\exp\left(-\frac{c_\perp}{2\mu}t\right)\cos\left(\sqrt{\alpha_n\frac{EI}{\mu} - \left(\frac{c_\perp}{2\mu}\right)^2}\,t - \delta_n\right), & n > n_c \end{cases} \quad (7)$$

where $n_c = \lfloor\frac{L}{\pi}\left(\frac{\mu}{EI}\right)^{1/4}\left(\frac{c_\perp}{2\mu}\right)^{1/2}\rfloor$ is the integral part[4] of $\frac{L}{\pi}\left(\frac{\mu}{EI}\right)^{1/4}\left(\frac{c_\perp}{2\mu}\right)^{1/2}$ and A_n, B_n, C_n, and δ_n can be found from the initial conditions imposed on the filament.

Thus using Eq. 6 for the spatial part and using Eq. 7 for the temporal part of the function, we construct the following equation as a solution of the homogeneous part of the filament equation:

$$y_c(x,t) = \sum_{n=1}^{\infty} y_{c_n}(x,t) = \sum_{n=1}^{\infty} X_n(x)Y_{c_n}(t). \quad (8)$$

Part 2: particular solution for a filament driven by a sinusoidal plane wave

In this section we solve the beam equation for a filament that is driven by a sinusoidal ultrasound wave. To do that, we first look for a particular solution of Eq. 1. Unfortunately, the method of separation of variables cannot be used directly, because the driving force does not depend on the spatial variable. Therefore, we assume that the driving

[2] This amplitude is proportional to the amplitude of the ultrasound at the location of the filament, which is related to the intensity of the wave at the location of the filament. In this section we are not interested in calculating this quantity since our solutions are proportional to A and we have good control of it through the intensity of the wave. This issue will be revisited in a later section.

[3] In fact, there is a third special situation, but here we have assumed that $\alpha_n EI/\mu \neq (c_\perp/2\mu)^2$. In the case of the critically damped solution, $\alpha_n EI/\mu = (c_\perp/2\mu)^2$, we have to add another term to the solution in Eq. 8

[4] This is also called an integral value or floor function (usually denoted this way in mathematics). In mathematics and computer science, the floor functions map a real number to the next smallest integer. More precisely, floor(x) is the largest integer not greater than x.

force is $AX(x)\sin(\omega t)$, instead of $A\sin(\omega t)$ as a first attempt to find a particular solution. This will help us solve the differential equation using the method of separation of variables. Later in this section we discuss the reasons for accepting this assumption and show that this is not a limitation of the method.

Substituting Eq. 2 into Eq. 1 with the new driving force and dividing the result by $X(x)Y(t)$ we again generate two eigenvalue equations. The eigenvalue equation related to the spatial part is the same as Eq. 3, and the eigenvalue equation related to the temporal part is

$$\frac{d^2Y(t)}{dt^2}+\frac{c_\perp}{\mu}\frac{dY(t)}{dt}+\alpha\frac{EI}{\mu}Y(t)=\frac{EIA}{\mu}\sin(\omega t). \tag{9}$$

Again, applying the initial conditions mentioned in Eq. 5 into Eq. 3, we find the the same eigenfunctions and eigenvalues as in Eq. 6. For the temporal function we try (Marion 1970) $D\sin(\omega t-\delta)$ as a particular solution. Substituting this function into Eq. 9, expanding $\sin(\omega t-\delta)$ and $\cos(\omega t-\delta)$, and using the fact that $\sin\omega t$ and $\cos\omega t$ are linearly independent, we find D and δ. Consequently, the particular solution is

$$Y(t)=\frac{\frac{EIA}{\mu}}{\left[\left(\alpha\frac{EI}{\mu}-\omega^2\right)^2+4\left(\frac{c_\perp}{2\mu}\right)^2\omega^2\right]^{1/2}}\sin(\omega t-\delta), \tag{10}$$

where δ in Eq. 10 is

$$\delta=\tan^{-1}\left(\frac{\frac{c_\perp}{\mu}\omega}{\alpha\frac{EI}{\mu}-\omega^2}\right). \tag{11}$$

This is the particular solution for the temporal part of the filament equation that represents all the information for large[5] t. Using Eq. 6 for the spatial function and Eq. 10 for the temporal function, we find the complete form of the particular solution for the filament vibration as

$$\begin{aligned}y_p(x,t)&=\sum_{n=1}^{\infty}y_{p_n}(x,t)=\sum_{n=1}^{\infty}B_nX_n(x)Y_{p_n}(t)\\&=\sum_{n=1}^{\infty}B_n\sin(\alpha_n^{1/4}x)\frac{\frac{EIA}{\mu}}{\left[\left(\alpha_n\frac{EI}{\mu}-\omega^2\right)^2+4\left(\frac{c_\perp}{2\mu}\right)^2\omega^2\right]^{1/2}}\\&\quad\times\sin(\omega t-\delta_n).\end{aligned} \tag{12}$$

Note that α_n has been calculated in Eq. 6. B_n can be found from the space dependence of the driving force.

So far, we found the particular solution for the nonhomogeneous term of $AX(x)\sin(\omega t)$ instead of $A\sin(\omega t)$. We now revisit the assumption made in order to use the method of separation of variables for the original filament equation. Since we know the eigenfunctions of Eq. 3, $X_n(x)$, produce a complete (or closed) set over the domain of]0,L[, this means that we can expand any spatial function on the right-hand side of Eq. 1 in terms of a linear combination of these eigenfunctions. Since the beam equation is also linear, particular solution for any spatial function present in the driving force term will be a linear combination of terms in Eq. 12 with the same coefficient B_n. To find B_n for the original problem, when the the nonhomogeneous term is $A\sin(\omega t)$, we just need to expand the numeral one over the domain of]0,L[in terms of eigenfunctions $X_n(x)$. Doing that we find (Arfken and Weber 2001; Appendix)

$$1=\frac{4}{\pi}\left[\frac{\sin(\pi x/L)}{1}+\frac{\sin(3\pi x/L)}{3}+\frac{\sin(5\pi x/L)}{5}+\cdots\right]. \tag{13}$$

Using the coefficients in the above expansion, substituting them into Eq. 12 and simplifying the result, we derive the following exact particular solution of the filament equation with a nonhomogeneous term $A\sin(\omega t)$,

$$\begin{aligned}y_p(x,t)=&\sum_{n=1,\text{odd}}^{\infty}\frac{4A}{n\pi\left[\left(n^4\left(\frac{\pi}{L}\right)^4-\frac{\mu}{EI}\omega^2\right)^2+\left(\frac{c_\perp}{EI}\right)^2\omega^2\right]^{1/2}}\\&\times\sin(n\pi x/L)\sin(\omega t-\delta_n).\end{aligned} \tag{14}$$

Now that we have found the exact particular solution for the filament equation driven by an ultrasound plane wave and we know that this term becomes the only important term just after a few oscillations of the filament subjected to ultrasound, we are ready to evaluate any physical quantity of interest.

Maximum bending and the resonance condition

In this section we first calculate the bending moment exerted on the cross-section of the filament. The reason for this calculation is that the bending moment is the quantity responsible for bending any beam or filament and if it exceeds some critical value (for a given filament with a particular cross-section and material type), the filament will break. Using the moment-curvature relationship, $M=EI/\rho$ (Segel 1987), and the small deflection approximation, $1/\rho=\partial^2 y(x,t)/\partial x^2$, we find the bending moment by taking a partial derivative of a particular solution with respect to x,

$$\begin{aligned}M(x,t)=&\sum_{n=1,\text{odd}}^{\infty}\frac{-4\left(\frac{n\pi}{L}\right)^2EIA}{n\pi\left[\left(n^4\left(\frac{\pi}{L}\right)^4-\frac{\mu}{EI}\omega^2\right)^2+\left(\frac{c_\perp}{EI}\right)^2\omega^2\right]^{1/2}}\\&\times\sin(n\pi x/L)\sin(\omega t-\delta_n).\end{aligned} \tag{15}$$

We then search for the frequencies that maximize the bending moment for each mode. To do that, we maximize the

[5] Here, "large" means large compared to the inverse of damping parameter, $c_\perp/2\mu$, in the complementary solution in Eq. 7. This means that for $t\gg 2\mu/c_\perp$ our solution can be demonstrated by the particular solution.

amplitude of the bending moment with respect to frequency. Taking the derivative of each of the amplitude of the bending moment in Eq. 15 with respect to ω and setting them to zero gives the frequencies that we seek, namely

$$\omega_n = 2\pi\nu_n = \left[\left(\frac{n\pi}{L}\right)^4 \frac{EI}{\mu} - 2\left(\frac{c_\perp}{2\mu}\right)^2\right]^{1/2}, \tag{16}$$

where ω and ν represent angular and linear frequency, respectively. Note that according to the above equation resonance occurs for the values of n that make the quantity under the square root positive. Solving the above equation for the smallest integer value of n that yields the real value for the frequency, n_0, we find the first resonant mode number as[6]

$$n_0 = \lceil \frac{L}{\pi}(\frac{\mu}{2EI})^{1/4}(\frac{c_\perp}{\mu})^{1/2} \rceil. \tag{17}$$

The reason for calling the above frequencies resonant frequencies is that they are the same frequencies that maximize the amplitudes in the filament equation (Eq. 14). When the amplitude in the filament equation is at a maximum for each frequency, the corresponding mode absorbs the maximum amount of energy from the source. This then defines a resonant frequency.

Analytical results

In this section we substitute physical parameter values for the MT into the obtained solution. Figure 2 (left axis) shows the graph of the resonant frequency as a function of the mode number for an MT with a length of 10 μm that is placed in an aqueous solution. The viscosity of the solution is 10^{-3} Pa·s (Howard 2001) and the diameter and flexural rigidity of an MT are equal to 25 nm and 3×10^{-23} N·m^2, respectively (Kikumoto et al. 2006; Kurachi et al. 1995). The mass of each tubulin dimer is considered to be 110 KDa. We also need to calculate $c_\perp$ (Howard 2001; Samarbakhsh and Tuszynski 2009), assuming the MT is far from the boundary of the solution, using the following equation :

$$F_\perp = \frac{4\pi\eta L}{\ln(\frac{L}{2r}) + 0.84} v, \tag{18}$$

where $F_\perp$ is the perpendicular component of the viscous force exerted on the MT by the solution when it moves with velocity v with respect to the solution. Here, η is the viscosity of the solution and L and r are the length and radius of the filament, respectively. As can be seen from the graph, the first resonance occurs at the mode number equal to 67, while for mode numbers below this value there is no resonance and the amplitude of the bending moment decreases monotonically as a function of frequency.

[6] "⌈⌉" in Eq. 17 is called a celling function that maps the argument to the next largest integer. Also note that in this section n must be an odd number and if we end up with an even number for n_0 in Eq. 17, we should take the next integer which is definitely an odd number.

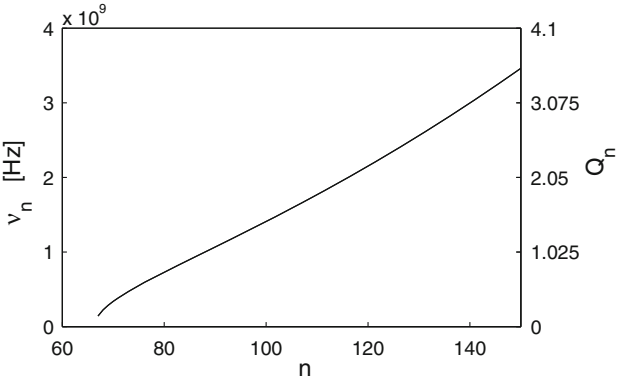

Fig. 2 The *left axis* shows a plot of the resonant frequency as a function of the mode number for a 10 μm length microtubule placed in the aqueous solution. The *right axis* shows a plot of the quality factor of resonance as a function of the mode number for the same microtubule

Figure 3 shows the amplitude of the bending moment (more precisely, it is the amplitude of the bending moment divided by EIA, but as explained in footnote 2, in this section we are only interested in maximizing the amplitude of the bending moment for a constant A, which is related to the intensity of the ultrasound at the location of the MT) at each resonant frequency as a function of the mode number. As can be seen from the graph, the amplitude decreases with an increasing mode number, which suggests that using the first resonant mode transfers the maximum amount of energy to the MT compared with other resonant modes. We

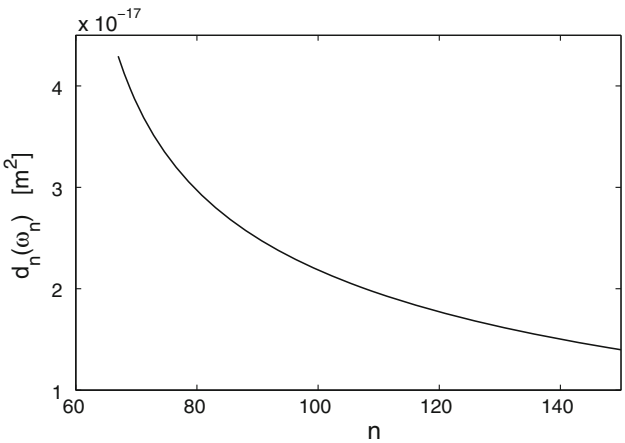

Fig. 3 A plot of the amplitude of the bending moment divided by EIA at each resonant frequency as a function of the mode number for a 10 μm length microtubule in an aqueous solution. In the graph, $d_n(\omega)$ is equal to $D_n(\omega)/EIA = 4(\frac{n\pi}{L})^2/n\pi[(n^4(\frac{\pi}{L})^4 - \frac{\mu}{EI}\omega^2)^2 + (\frac{c_\perp}{EI})^2\omega^2]^{1/2}$ and in order to obtain the graph, we should substitute ω_n from Eq. 16 in $d_n(\omega)$

discuss this later in regard to the quality factor of each mode.

Figure 4 shows the amplitudes of the bending moment as a function of frequency for three different modes. As can be seen, the amplitude at the resonant frequency for these modes, which occurs at a maximum of the curves, decreases with an increasing mode number. This is also clear from Fig. 3, but here we bring the reader's attention to the fact that although the amplitude at the resonant frequency decreases with an increasing mode number, the width of the curves decreases faster in such a way that *Quality factor*, Q-factor, of the resonance, which describes the sharpness of each resonance (here Q-factor is equal to $\mu\omega_n/c_\perp$), increases with increasing mode number. Unlike the amplitude that suggests to use the first resonant mode to transfer the maximum amount of energy to the MT, Q-factor suggests that for a sharper resonance we should use modes with a higher mode number. We will resolve this issue in the next section by introducing a single mode excitation of the MT. Figure 2 (right axis) shows the quality factor as a function of the mode number.

Although we have solved and discussed the resonance condition, the amplitude of the bending moment at each resonant frequency, and the Q-factor of each mode, it should be noted that when the MT is driven by an ultrasound plane wave, the solution will be a linear combination of all modes in Eq. 15. More specifically, when we discussed the resonant frequency for one specific mode, we really meant the contribution of that mode when the filament is driven by a specific frequency is at a maximum compared to its contribution when the filament is driven by any other frequency. However, an MT actually vibrates

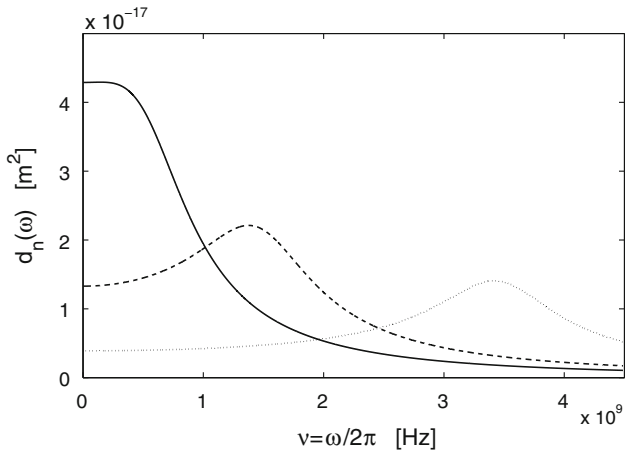

Fig. 4 A plot of the amplitudes of the bending moment divided by *EIA* for a 10 μm length microtubule in an aqueous solution as a function of frequency for three different modes. (1) the *solid curve* for the mode number equal to 67 (which corresponds to the first resonant mode, n_0), (2) the *dashed curve* for the mode number equal to 99, and (3) the *dotted curve* for the mode number equal to 149

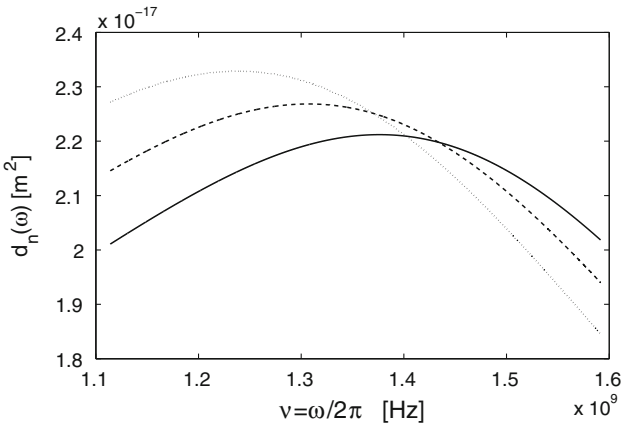

Fig. 5 A plot of the amplitudes of the bending moment divided by *EIA* for the same microtubule as a function of frequency for three consecutive modes:(1) the *solid curve* for the mode number equal to 99, (2) the *dashed curve* for the mode number equal to 97, and (3) the *dotted curve* for the mode number equal to 95

with a combination of all of its eigen modes. Some of the modes with a lower mode number may not satisfy the resonance condition but have a larger amplitude than the amplitude of the specific mode.

Figure 5 clearly illustrates the previous paragraph. Although the mode number 99 is at resonance (the solid curve at its peak), the amplitudes of the mode number 97 (dashed curve) and 95 (dotted curve) are still higher than the amplitude of this mode at its resonant frequency. This proves that the ultrasound plane waves really do not establish any resonance condition for the MT.

Single mode excitation

In order to control the system with frequency, we have to excite just one single mode whose mode number is larger that n_0 (in order to achieve resonance) and eliminate all other modes. To do that we can no longer excite the filament with an ultrasound plane wave as considered before but instead need to modulate the wave. Reviewing carefully the steps taken to reach the solution in Eq. 14 helps us find out what kind of modulation should be attempted for this purpose. To eliminate the other modes and to excite only a single mode[7], say m, we should eliminate the other terms in the summation in Eq. 15. However, we know that the summation has come from the expansion of the numeral one, in terms of $\sin(n\pi x/L)$ (in order to produce the plane wave). This explains why we cannot excite the filament with a plane wave anymore and guides us

[7] In this paper, we use m as a mode number when we excite a single mode and eliminate the other modes (refer to Eqs. 19 and 20). Here, n has been used to label the mode number for excitation of a single mode by an ultrasound plane wave (refer to Eqs. 14 and 15).

to excite the filament with a force density of the form $EIA\sin(m\pi x/L)\sin(\omega t)$ instead of $EIA\sin(\omega t)$.

Using the above force density, the solution for the filament vibrational equation and the bending moment equation can be found from the following equations, respectively

$$y_p(x,t) = \frac{A}{[(m^4(\frac{\pi}{L})^4 - \frac{\mu}{EI}\omega^2)^2 + (\frac{c_\perp}{EI})^2\omega^2]^{1/2}} \times \sin(m\pi x/L)\sin(\omega t - \delta_m), \quad (19)$$

$$M(x,t) = \frac{-(\frac{m\pi}{L})^2 EIA}{[(m^4(\frac{\pi}{L})^4 - \frac{\mu}{EI}\omega^2)^2 + (\frac{c_\perp}{EI})^2\omega^2]^{1/2}} \times \sin(m\pi x/L)\sin(\omega t - \delta_m). \quad (20)$$

In Fig. 6, we have shown a plot of the amplitudes of the bending moment divided by *EIA* for a 10 μm length MT in an aqueous solution. Comparing this figure with Fig. 4 reveals two major advantages of the excitation of a single mode of the filament with the modulated wave of $EIA\sin(m\pi x/L)\sin(\omega t)$ with respect to the excitation by a plane wave. First, the amplitude is much larger in Fig. 6 (specifically, it is $m\pi/4$ times larger since we do not need to expand the plane wave in terms of harmonic modes). The second advantage is that by increasing the mode number, m, the amount of the amplitude of the bending moment at a resonant frequency (the maximum of each curve) does not drop as fast as in Fig. 4 and becomes almost flat for a large mode number.

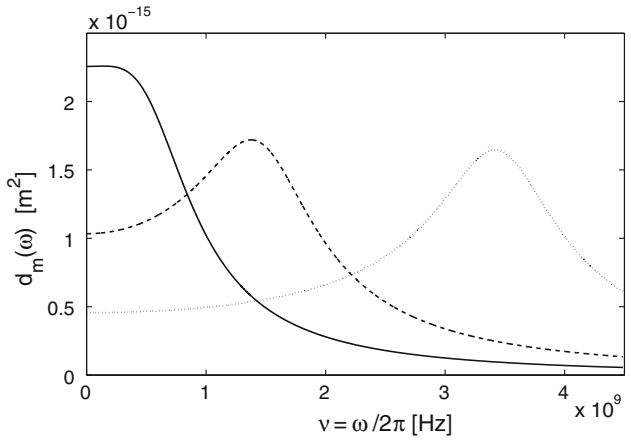

Fig. 6 A plot of the amplitudes of the bending moment divided by *EIA* for a 10 μm length microtubule when a single mode is excited at a time as a function of frequency, for three modes: (1) the *solid curve* for $m = 67$, (2) the *dashed curve* for $m = 99$, and (3) the *dotted curve* for the mode number equal to $m = 149$. Note that there is no need to pick the odd mode number when we excite just a single mode and eliminate the other modes. Here, we selected the same mode number shown in Fig. 4 in order to compare the two situations accurately. Also note that, unlike in Fig. 4 where the curve is shown for any driving frequency (since the filament was excited with a plane wave), here a single mode of the system was excited at a time with a driving force density of the form $EIA\sin(m\pi x/L)\sin(\omega t)$.

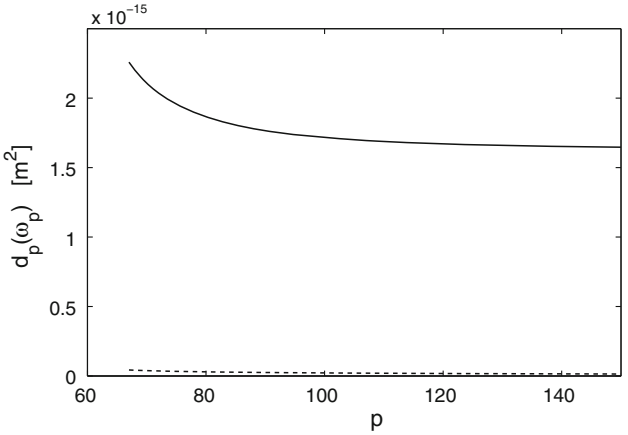

Fig. 7 A plot of the amplitude of the bending moment at each resonant frequency divided by *EIA* as a function of the mode number for a 10 μm length microtubule in an aqueous solution. The *solid curve* (replacing p with m) shows excitation with a modulated wave of $EIA\sin(m\pi x/L)\sin(\omega t)$. The *dashed curve* (replacing p with n) shows excitation with a plane wave having the same amplitude

This is more clear in Fig. 7, which shows a plot of the amplitude of the bending moment divided by *EIA* at each resonant frequency as a function of the mode number for the same filament for both kinds of excitations. As can be seen, not only does the modulated excitation yield a much larger amplitude but also the size of the amplitude for a large mode number is almost independent of the mode number. The graph of the Q-factor as a function of the mode number remains exactly the same as the excitation using the plane wave in Fig. 2. As with the modulated excitation, there is no decrease of the amplitude with increasing mode number. These two graphs (Figs. 2 and 7) suggest that for more control over the system, we should use higher mode numbers.

Therefore, the above results lead to the conclusion that we should excite just a single mode of the MT with a modulated wave of the form of $\sin(m\pi x/L)\sin(\omega t)$.

From the theoretical point of view, we have demonstrated that in order to have frequency control over vibrations of the filament we should excite just one single mode of the filament, but this still leaves the issue of an experimental implementation of this idea. Is there a device that could produce such a modulated wave?

While presenting technical solutions to such experimental issues is outside the scope of this paper and providing answers to the above questions is best left to experimentalists, we still intend to broadly outline a direction that, in our opinion, should be taken in future experimental work. Potentially, a piezoelectric transducer such as PZT-8 ceramics (Prabakar and Mallikarjun Rao 2006) can produce a relevant range of frequencies (although a tiny space variation may pose a challenge), but here we wish to present an idea for its potential implementation. We think that a design involving

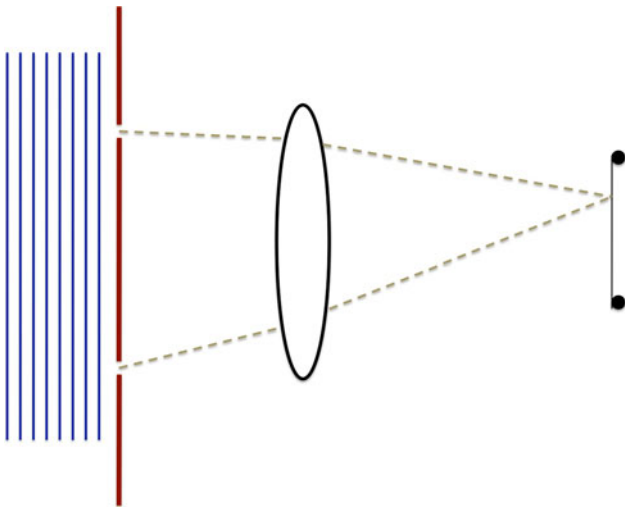

Fig. 8 A schematic of the proposed double slit ultrasound device for a single mode excitation (figure not to scale)

interference and double slit effects can lead to successful solutions of the problems addressed above. An ultrasound plane wave passing through a double slit can produce a modulated wave needed for single mode excitation. Figure 8 shows a schematic of such a device. The reason for putting an acoustic lens between the double slit and the filament is to enable the control of the distance between two adjacent maxima. Without this lens it seems impossible to produce such a minute separation between two adjacent maxima as required by the design principle. To better elucidate this issue, we now illustrate it with some concrete numbers. As an example, we assume the distance between two slits and the distance between the double slit and the filament are 1 mm and 1 cm, respectively. For a resonant frequency of about 1.5 GHz, which approximately corresponds to the mode number 100, and taking into account the speed of sound in an aqueous solution being about 1,500 m/s, we find the value of about 10 μm giving the distance between two adjacent maxima. This is almost 100 times larger than the distance between two adjacent maxima needed for mode number 100 for an MT as presented in this paper. However, we still need an acoustic lens to reduce this distance to the correct value.

Intensity and sound level estimation

In this section we calculate the minimum requirement on the ultrasound intensity to break an MT. In order to break an MT, we should bend it to a minimum local curvature. Odde et al. (1999) provides useful information about the breakage of MTs. The mean curvature to break an MT in Waterman-Storer and Salmon's (1997) report is around 1.7 rad/μm. In a paper published later, Odde et al. (1999) reported 1.5 rad/μm for the related mean curvature. Substituting this curvature value and flexural rigidity of an MT into the moment-curvature relationship, we can calculate the *minimum required bending moment* exerted on the cross-section of an MT to break it. This value is about 4.5×10^{-17} N·m and is denoted by M_B in what follows. Note that we should equate M_B with the maximum of the bending moment in Eq. 20, which is simply the amplitude of the bending moment in this equation, to find the relation between M_B and the *minimum required ultrasound intensity* (denoted by I_B in the rest of this section). This will be demonstrated below. Also, as the maximum bending moment corresponds to the maximum of the MT solution in Eq. 19, we conclude that the breakage of MTs occurs at the locations of antinodes.

As mentioned in the section "Derivation of vibrational dynamics equations," *EIA* is the amplitude of the force density. This quantity is related to the *pressure amplitude* of ultrasound through the simple relation between the force and pressure,

$$EIA = 2r\Delta p_0, \tag{21}$$

where Δp_0 and r denote the pressure amplitude, which is the maximum increase or decrease in pressure due to ultrasound, and the radius of MT, respectively. Pressure amplitude is related to the *displacement amplitude*, which is the maximum displacement of the fluid element to either side of its equilibrium position, through the following formula (Halliday et al. 2000):

$$\Delta p_0 = v\rho_s\omega s_0, \tag{22}$$

where v, ρ_s, ω, and s_0 denote the speed of sound in solution (Kinsler et al. 2001), density of the solution, angular frequency of ultrasound, and the displacement amplitude, respectively. By eliminating Δp_0 between Eqs. 21 and 22, and solving for s_0, we obtain the following equation for the displacement amplitude,

$$s_0 = \frac{EIA}{2rv\rho_s\omega}. \tag{23}$$

So far, we have managed to find the relationship between the displacement amplitude, hence the sound intensity, and the force density amplitude. In order to obtain an estimate for I_B, we first need to find the relation between the bending moment and force density amplitude. This is achieved by analyzing Eq. 20, in order to relate M_B and EIA_B. Namely,

$$\begin{aligned} M_B &= D_m(\omega) = d_m(\omega)EIA_B \\ &= \frac{\left(\frac{m\pi}{L}\right)^2}{\left[\left(m^4\left(\frac{\pi}{L}\right)^4 - \frac{\mu}{EI}\omega^2\right)^2 + \left(\frac{c_\perp}{EI}\right)^2\omega^2\right]^{1/2}} EIA_B. \end{aligned} \tag{24}$$

Substituting the above relation for EIA_B into Eq. 23 gives the *minimum required displacement amplitude*, s_{0B}, to break an MT,

$$s_{0B} = \frac{M_B}{2rv\rho_s\omega d_m(\omega)}. \quad (25)$$

Finally, using the relation between intensity and the pressure amplitude of sound (Halliday et al. 2000), we obtain

$$\text{Intensity} = \frac{1}{2}\rho_s v\omega^2 s_0^2. \quad (26)$$

We now find the final formula for the minimum required ultrasound intensity to break an MT as

$$I_B = \frac{1}{2v\rho_s}\left[\frac{M_B}{2rd_m(\omega)}\right]^2. \quad (27)$$

At this point, we substitute physical values for the parameters in Eq. 27 to estimate I_B for a 10 μm length MT in an aqueous solution. M_B was estimated at the beginning of this section. Using Fig. 6 to evaluate $d_m(\omega_m)$ for the mode numbers 67, 99, and 149, we find 213, 363, and 397 KW/m^2 for I_B, respectively. These intensities correspond to decibel values of 173.3, 175.6, and 176.0 dB, respectively. These theoretical predictions should be relatively straight-forward to validate experimentally.

Discussion and conclusions

In this paper, by introducing a new method, we solved the beam equation for a uniform bio- and nano-filament placed in a viscous solution, attached at its two ends, and driven by ultrasound plane waves. The method is based on converting the related beam equation to an equation that allows the use of the method of separation of variables. We then reconstructed the solution of the original beam equation from the solutions of the converted equations. Moreover, we have used the parametric equations found in this paper to investigate the resonance condition for an MT in an aqueous solution. Needless to say, achieving resonance is important in order to control the transfer of energy to the MT and to attain its maximum rate. We have shown that the ultrasound plane wave cannot satisfy the resonance condition for the MT as it excites all the odd-number modes at the same time. We have also shown that in order to achieve resonance we should excite only a single mode of the MT. Single mode excitation results in a noticeable reduction (by four orders of magnitude) of the total energy transferred to the surrounding medium since it requires a much smaller sound intensity compared to the multi-mode excitation. Another important result presented in this paper is the fact that the amplitude of the bending moment is almost independent of the mode number in single mode excitation. This will help excite a higher mode in order to achieve the resonance condition with a high quality factor and a high amplitude at the same time.

Another aspect that we wish to briefly discuss here is the dependence of the first resonant mode number on the length of the filament. As can be seen from Eq. 17, for filaments with $L \ll 1$ m (which for bio- and nano-filaments is always the case), $\lceil \frac{1}{\pi}(\frac{\mu}{2EI})^{1/4}(\frac{c_\perp}{\mu})^{1/2} \rceil \approx \frac{1}{\pi}(\frac{\mu}{2EI})^{1/4}(\frac{c_\perp}{\mu})^{1/2}$. This means that the first resonant mode number is proportional to the length of the filament and subsequently the ratio of L/n_0 is independent of L. This ratio defines the maximum possible distance between two neighboring nodes and it does not depend on the length of the filament. For example, in the case of a 5 μm long MT (i.e., half of 10 μm), we readily conclude that the first resonant mode number is $67/2 = 34$ which is found by a scaling rule. Also, Eq. 16 indicates that for a given possible mode number, resonance frequency decreases with increasing length of the filament.

Furthermore, the dependence of the first resonant mode number and resonance frequencies on the viscosity of the solution is important. We have assumed in this study that it applies to an experimental set up in vitro, where MTs are typically submerged in a buffer solution whose viscosity is close to the viscosity of water. In the case of an arbitrary viscosity, since the equations derived for the first mode number and resonant frequencies are completely analytic and parametric, we can substitute the related values for the arbitrary viscosity into these equations and extract the relevant solutions corresponding to these viscosities. For example, in the case of the actual cytoplasmic viscosity, which is about 10 times greater than the viscosity of water (Salmon et al. 1984), using Eq. 17 results in the first mode number increasing by a factor of $10^{1/2} \approx 3$. The corresponding relation for the resonant frequencies is a little more complicated through Eq. 16, but this equation shows that the resonant frequency for a given mode number will decrease. The complexity involved in the rheology of the entire cell appears to be outside the scope of this manuscript. In the future, the scope of this work should go beyond individual filaments towards integrating cell mechanics (Fabry et al. 2001).

In recent experiments (Pizzi and Fiorentini (2009); Pizzi et al. (2011)) solutions containing assembled and unassembled tubulin were subjected to waves produced by a microwave generator in the range between 0.8 and 2.5 GHz. While the spectrum analyzer detected no significant changes in the case of free tubulin in solution and the control buffer solution with no protein, samples containing microtubules in solution showed a resonance phenomenon centered at 1.51 GHz. This was interpreted as indicating resonant absorption of electromagnetic energy at a frequency range within that predicted in this paper. The authors suggested a mechanical mode of behavior in the case of microtubules, as opposed to free tubulin of buffer

solution, a conclusion that is consistent with our analysis. Another recent experiment (Pokorny et al. 2011) also reported resonant energy absorption of MTs within the range of GHz excitations.

Finally, by finding a new parametric equation describing the breakage intensity of bio- and nano-filaments in a viscous fluid and subjected to ultrasound, we have estimated the required minimum breakage intensity for the ultrasound at the location of an MT. We have shown that for a 10 μm MT in an aqueous solution, this intensity is on the order of 10^5 W/m^2, which corresponds to 170 dB.

Acknowledgments A.S. wishes to thank Neda Naseri and Laleh Samarbakhsh for their assistance. This research was supported by grants from the Natural Sciences and Engineering Research Council of Canada, the Alberta Cancer Foundation, and the Allard Foundation.

Appendix: expansion coefficients in Eq. 13

Here we calculate the coefficients of the Fourier sine series for the following function in the interval]0, L[

$$f(x) = \begin{cases} -1 & -L < x < 0 \\ 0 & x = 0 \\ 1 & 0 < x < L \end{cases} \tag{A1}$$

Coefficients pre-multiplying the cosine terms are

$$a_n = \frac{1}{L}\left(-\int_{-L}^{0} \cos\left(\frac{n\pi s}{L}\right) \mathrm{d}s + \int_{0}^{L} \cos\left(\frac{n\pi s}{L}\right) \mathrm{d}s \right) = 0 \tag{A2}$$

which is obvious as the above function is an odd function.

Also the coefficients for sine terms are

$$\begin{aligned} b_n &= \frac{1}{L}\left(-\int_{-L}^{0} \sin\left(\frac{n\pi s}{L}\right) \mathrm{d}s + \int_{0}^{L} \sin\left(\frac{n\pi s}{L}\right) \mathrm{d}s \right) \\ &= \begin{cases} 4/n\pi & n \text{ is an odd number} \\ 0 & n \text{ is an even number} \end{cases} \end{aligned} \tag{A3}$$

Using the above equations we obtain $\frac{4}{\pi}[\sin(\pi x/L)/1 + \sin(3\pi x/L)/3 + \sin(5\pi x/L)/5 + \cdots] = 1$ for $0 < x < L$.

References

Arfken GB, Weber HJ (2001) Mathematical methods for physicists, 5th edn. Harcourt/Academic, San Diego
Fabry B, Maksym GN, Butler JP, Glogauer M, Navajas D, Fredberg JJ (2001) Phys Rev Lett 87:148102
Gere JM, Timoshenko SP (1991) Mechanics of materials, 3rd SI edn. Chapman and Hall, London
Halliday D, Resnick R, Walker J (2000) Fundamental of physics, 6 edn. Wiley, New York
Howard J (2001) Mechanics of motor proteins and the cytoskeleton. Sinauer, Sunderland
Hrazdira I, Skorpikova J, Dolnikova M (1998) Eur J Ultrasound 8:43–49
Kennedy JE, ter Haar GR, Cranston D (2003) Br J Radiol 76:590–599
Kikumoto M, Kurachi M, Tosa V, Tashiro H (2006) Biophys J 90:1687–1696
Kinsler LE, Frey AR, Coppens AB, Sanders JV (2001) Fundamentals of acoustics, 4th edn. Wiley, New York
Kurachi M, Hoshi M, Tashiro H (1995) Cell Motil Cytoskelet 30:221–228
Marion JB (1970) Classical dynamics of particles and systems, 2nd ed. Academic Press, New York
McDonald KT (2000) Am J Phys 68:486–488
Miller MW, Miller DL, Brayman AA (1996) Ultrasound Med Biol 22(9):1131–1154
Neuman KC, Block SM (2004) Rev Sci Instrum 75:2787–2809
Odde DJ, Ma L, Briggs AH, Demarco A, Kirschner MW (1999) J Cell Sci 112:3283–3288
Pizzi R, Fiorentini S (2009) Proceedings of the 9th WSEAS international conference on applied computer science. WSEAS, Stevens Point, WI
Pizzi R, Strini G, Fiorentini S, Pappalardo V, Pregnolato M (2011) Artificial neural networks. Nova Publishers, New York
Pokorny J, Vedruccio C, Cifra M, Kucera O (2011) Eur Biophys J 40:747–759
Prabakar K, Mallikarjun Rao SP (2006) J Phys D Appl Phys 39:2433
Rao SS (2004) Mechanical vibration, 4th edn. Pearson Prentice Hall, Upper Saddle River
Salmon ED, Saxton WM, Leslie RJ, Karow ML, McIntosh JR (1984) J Cell Biol 99:2157–2164
Samarbakhsh A, Tuszynski JA (2009) Phys Rev E 80:011903
Segel LA (1987) Mathematics applied to continuum mechanics. Dover, New York
Spadoni A, Daraio C (2010) PNAS 107:7230–7234
Waterman-Storer CM, Salmon ED (1997) J Cell Biol 139:417–434
Wu F, Wang Z, Zhu H, Chen W, Bai J, Li K, Jin C, Xie F, Su H (2005) Radiology 236:1034–1040